Cronfa - Swansea University Open Access Repository

_____

This is an author produced version of a paper published in:
Separation and purification technology

_____

Cronfa URL for this paper:

_____

Paper:

_____

Dewatering of POME digestate using lignosulfonate driven forward osmosis

Daniel Johnson[1], Ang Wei Lun[2], Abdul Wahab Mohammed[2] and Nidal Hilal[1,3]*

1. *Centre for Water Advanced Technologies and Environmental Research (CWATER), College of Engineering, Swansea University, Swansea SA2 8PP, United Kingdom*

2. *Centre for Sustainable Process Technology (CESPRO), Faculty of Engineering and Built Environment, Universiti Kebangsaan Malaysia, 43600 Bangi, Selangor Darul Ehsan, Malaysia*

3. *NYUAD Water Research Center, New York University Abu Dhabi, Abu Dhabi, United Arab Emirates*

* Corresponding author, email: n.hilal@swansea.ac.uk

Highlights

- Lignosulfonates investigated as draw solutes for de-watering of POME Digestate

- Na Lignosulfonate had higher water flux than Ca lignosulfonate draw solution

- Na Lignosulfonate showed lower reverse solute flux than Ca lignosulfonate or NaCl solutions

- Osmotic pressures of solutions directly measured by dead-end filtration method

- Osmotic pressure of POME digestate measured at 1.58 bar

Keywords

Forward osmosis, palm oil mill effluent, POME dewatering, membrane technology, lignosulfonate

Abstract

High demand for palm oil results in the production of huge quantities of palm oil mill effluent (POME) wastewater containing a high amount of organics. Currently, this is often processed by anaerobic fermentation, but the waste water still requires further processing. Dewatering of POME digestate could simultaneously recover nutrients for use as organic fertiliser and treat water sufficiently to allow other uses. This work investigates the feasibility of using a forward osmosis (FO) process driven by lignosulfonate draw solutions. It was found that water fluxes for pure water and simulated POME

digestate feeds were lower for lignosulfonates than NaCl as draw solutes, but had much lower reverse solute fluxes. Reverse solute flux is of great importance for dewatering of POME digestate, as concentration of salts in the dewatered feed will preclude their use as organic fertilisers. Na lignosulfonate showed both higher water fluxes and lower reverse solute flux than the Ca lignosulfonate. Water fluxes when using the simulated POME digestate were lower than predicted from the directly measured osmotic pressures of the solutions, suggesting increased membrane resistance due to fouling or concentration polarisation effects. In addition, osmotic pressures of organic solutions were measured directly from dead-end filtration measurements. This showed that the relationship between osmolality measured from freezing point depression measurements and osmotic pressure of solutions varies for different solutes, suggesting that osmolality measurements do not give a reliable measure of osmotic pressure when comparing different organic solutions.

1.0 Introduction

Products derived from the commercial oil palm, *Elais guinieensis,* are of increasing economic importance in a number of developing countries [1], and are being used more and more widely, especially where consumers wish to replace animal derived fats with plant fats [2] and in the development of biologically derived fuels [3, 4]. The oil palm is capable of producing more oil per cultivated hectare than any other oil producing crop [5]. One drawback in the processing of palm oil is the large amount of water used, resulting in a large quantity of wastewater, commonly termed palm oil mill effluent (POME), which is produced in volumes three times that of the crude palm oil product itself [6]. POME contains a high organic content, and hence exhibits large values for biochemical and chemical oxygen demand, rendering it unsuitable for release into the environment without extensive treatment [6-9].

Conventional treatment with POME takes the form of discharging the wastewater into a series of treatment using anaerobic digestion followed by aerobic ponding. The treated wastewater is then further polished to comply with environmental regulations, or dried to allow resource recovery [10]. Much research has been carried out into reducing the organic content of POME by bacterial digestion to produce useful by-products, including methane and hydrogen gas [7]. However, this still leaves a digestate requiring further treatment [11]. Such treatments need to be environmentally friendly and cost competitive with rival technologies.

One emerging technology for the energy efficient treatment of contaminated waters is the process of forward osmosis (FO) [12-16]. FO operates on the principle that water will diffuse through a semi-permeable membrane from a lower concentration solution to a higher concentration solution. By using a draw solution of higher osmotic concentration than the waste water feed, modest flux rates can be achieved. This process alone requires much less power to operate than traditional pressure driven membrane processes, where the main energy requirement is in the high pressures needed to be applied on the feed side to attain acceptable water fluxes. In addition, due to the low hydraulic pressures used, membrane fouling is reduced, with the majority of fouling being recoverable with backwashing. However, there is a major drawback with FO, which is that the product is not pure water, but a diluted draw solution. Regeneration of the draw solution into a sufficiently concentrated form, whilst recovering clean water, requires a secondary process, such as reverse osmosis, ultrafiltration or membrane distillation, which increases the overall energy requirements. In many cases, this secondary process increases the energy costs of the overall system to greater than that of the optimal conventional treatment, rendering FO as a niche application [13, 17, 18]. To counter this drawback, much research has endeavoured to produce novel draw solutes with innovative low cost recovery routes, including tailored nanoparticles, polyelectrolytes and stimuli responsive hydrogels [19, 20]. One other alternative route is to find niche applications where the diluted draw solution can be used elsewhere, instead of being regenerated. The most prominent example is using inorganic fertilizers, with the diluted draw being applied to irrigation water for application to crops [21-25]. For

desalination this raises the question of where the irrigation water itself comes from, due to the 100 times dilution required [26], but for dewatering applications this is not necessarily an issue.

Another potential draw solute which does not necessarily need to be regenerated is sodium lignosulfonate (Na Lig), which has previously been investigated for seawater desalination in desert areas [27]. The researchers found that the Na Lig solutions were capable of having high osmotic pressures, generating reasonable water fluxes when using pure water or saline feeds, with concentrations of 600 g /kg Na Lig sufficient to remove water from saline solutions. Lignosulfonates have previously been shown to act as soil stabilisers, reducing erosion [28-30], and as such do not necessarily need to be regenerated after FO dilution, instead being applied directly to soils. Palm oil plantation soils are subject to erosion [31], with recent estimates for oil palm plantations putting soil losses at between 2.85 and 5.26 tonnes per hectare per year for flat surfaces [32], depending upon surface cover, with higher values of 78.5 tonnes per hectare possible depending upon soil type and surface gradient [31]. Therefore, it seems sensible that the diluted draw solution of lignosulfonates could potentially be applied to oil palm plantation soils, when combined with irrigation water, without further need for regeneration. Previous studies of soil stabilisation using lignosulfonate or lignin based solutions have found optimal spray concentrations of 2% by weight [33-35]/. Therefore, we propose in this work to investigate the potential of sodium and calcium based lignosulfonates (Na Lig and Ca Lig respectively) as potential draw agents for the dewatering of POME digestate using an FO process.

Due to the difficulty of obtaining POME digestate samples in sufficient quantities for bench scale research, it was decided to use humic acid (HA) solutions made up to the same osmotic concentration (osmol/kg) and pH as POME digestate as a simulated POME digestate for FO filtration experiments. Simulated solutions of this type also have the advantage of being well characterised and of consistent quality.

2.0 Experimental

2.1 Chemicals and Membranes

Dried Na Lig and Ca Lig was provided by Borregaard UK Ltd as dry powder, cas no. 8061-51-6, 8061-56-7 respectively. Samples were made up to the desired concentration by dissolving in deionised water. Anaerobically digested POME was obtained from a closed-type anaerobic digester system at SIME Darby East Palm Oil Mill, Carey Island, Malaysia, as previously reported [11]. POME digestate sample, HA and lignosulfonate solutions were filtered through a Grade 11 Ashless Fast Filtering Quantitative Filter Paper (Fisher Scientific, UK) to remove coarse particulate matter. Characteristics as previously reported are shown in table 1.

Humic acid (sodium salt) was obtained from Sigma Aldrich. For FO filtration measurements a simulated POME digestate was made using HA solution adjusted to the same pH and osmotic concentration as POME digestate. This allowed greater quantities of feed to be used than the availability of POME digestate and also ensured consistent feed water quality could be maintained. HA was dissolved in de-ionised water at the desired concentration. The pH was then adjusted to 7.6 using 0.1M HCl, before filtration to remove suspended undissolved particles. Finally the HA solution was diluted with deionised water until the same osmotic concentration, as determined by freezing point osmometry, as the POME sample was achieved, before filtering to remove any flocs.

All FO measurements were carried out using flat-sheet membranes supplied by Toray Chemical Korea Inc., Korea. These membranes have an asymmetric structure that is composed of three layers: 1 - polyamide coating as a selective layer on the top: 2 - an intermediate polysulfone porous substrate, and 3 - a polyester support mesh embedded in the polysulfone substrate providing mechanical strength [21].

2.2 Freezing Point Osmometry

Measurements of osmotic concentration of solutions was carried out by measurement of the freezing point depression of solutions using a Osmomat 030 Cryoscopic Osmometer (Gonotec GMBH). Cryoscopic osmometers measure the change in freezing point of an aqueous solution compared to that of pure water:

$$C_{osm} = \frac{\Delta T}{K}$$
(1)

where C_{osm} is the osmolality (osmol/kg), i.e. the molal concentration of all osmotically active components, ΔT is the freezing point depression (K) and K is a freezing point constant, determined from calibration with a solution of known concentration. Samples of 50 µl were transferred to suitable aliquots for measurement. The low volume needed allowed samples to be taken from feed and draw solutions during the FO tests to allow change in concentration to be monitored. However, K is not truly constant, and will vary depending on the concentration and composition of the solution. As such for complex mixtures of organics, the osmolality values may diverge from their true values[36]. In addition, calculating the actual osmotic pressure from osmolality values is non-trivial for a complex mixture of organics with unknown composition, such as wastewater. For this reason we decided to directly measure the osmotic pressure of organic solutions using membrane osmometry.

2.3 Membrane Osmometry

Water flux across a membrane during pressure driven filtration may be generalised by the following relationship:

$$J_w = A\,(\sigma\Delta\pi - \Delta P)$$
(2)

where J_w is water flux, A is the membrane water permeability, σ is the reflection coefficient, $\Delta\pi$ is the osmotic pressure difference across the membrane and ΔP is the hydraulic pressure difference across the membrane. It follows from this relationship that when the osmotic pressure and hydraulic pressure acting in opposite directions are of equal magnitude then $J_w = 0$. Therefore, a plot of Jw versus

ΔP should yield the value of $\Delta\pi$. If $\sigma=1$ and concentration polarisation effects are negligible then $\Delta\pi$ = solution osmotic pressure. This approach was previously demonstrated by Nabetani et al, who developed a membrane osmometer system based on this principle [37]. Determining osmotic pressure this way has an advantage over static membrane osmometers as not needing long wait times to allow equilibrium to be reached.

Osmotic pressures of solutions were measured directly using dead end filtration through an AK2540TM membrane (GE Power and Water), with a Sterlitech HP450 dead end filtration cell stirred using a magnetic stirrer set at 100 rpm for all measurements. Effective membrane area was 14.6 cm^2 and initial sample volumes of 250 ml were used. The system temperature was maintained at a constant 25 °C by siting the filtration cell in a water bath. Prior to all measurements, the membrane was flushed with de-ionised water at a pressure of 15 bar for 30 minutes to allow membrane compaction to occur and to remove preservatives. Fluids to be measured were placed in the filtration cell and pressure was increased using pressurised nitrogen gas. Mass flow was measured using an electronic balance connected to a computer. All samples were pre-filtered to remove any particulates which could potentially form cake layers on the membrane surface.

2.4 FO Filtration Rig and Test Procedure

A schematic of the set-up of the FO rig is shown in figure 1, as previously described [21]. The membrane filtration cell had dimensions of 16.6 cm x 8.6 cm with an effective membrane area of 8.4 cm^2. A hydrophilic sintered porous plastic spacer (BioVyon, Porvair, UK) was used to support each side of the membrane, which was oriented with the active layer facing the feed solution. The DS and FS on both sides of the membrane were circulated by two gear pumps in a cross-flow configuration. Flow rate was adjusted to 100 ml/min for all measurements, which produced a cross-flow velocity of 5.2 cm/s and the pressure was set at 0.2 bar on each side, with the

pressure continuously monitored and adjusted by needle valves downstream of the membrane cell to ensure a constant equal pressure on both sides. Initial volumes of feed and draw solutions were 1 litre for all measurements. The draw solution tank was placed on a weighing scale (Precisa, UK), with time and mass logged automatically on a computer. The temperature of both solutions was constant at 20.5 $^{\circ}$C during all experiments. The conductivity was measured by two calibrated conductivity meters (Jenway Man-Tech 4510 and HI-8734 Multi-range TDS Meter, HANNA instruments) placed in the draw and feed tanks, respectively. In addition, at 5 minute intervals 50 μl samples of solution were removed from each tank to allow osmolality measurements to be carried out.

Water flux, J_w, for FO and osmotic pressure measurements was calculated using the following equation from mass change measured on the balance:

$$J_w = \frac{\Delta V}{A_m \Delta t} = \frac{\Delta m}{A_m \, \Delta t \, \rho} \tag{3}$$

where ΔV is permeate volume change, Δt is time between measurements, A_m is effective membrane area, m is measured permeate mass and ρ is permeate density (assuming permeate density is approximately equal to that of pure water). On commencing measurements pressure was increased until permeate flow was observed in order to flush air out of the system. Pressure was then reduced to a lower value before increasing step wise in ten minute increments to allow flux to be measured at a range of applied pressures. This allowed plots of J_w versus ΔP to be constructed, with the x- intercept obtained from linear regression giving the value for the osmotic pressure of the solution.

For FO measurements with pure water feeds, the reverse solute flux, J_s can be calculated from changes in the feedwater concentration, as monitored by conductivity [38]:

$$J_s = \frac{(C_t V_t) - (C_0 V_0)}{A_m \, \Delta t} \tag{4}$$

where C_0, C_t are the feed concentrations (grams per litre) initially and after time Δt, V_0, V_t are feed volume initially and after Δt.

For fresh membranes, pure water on the feed and draw sides was allowed to flow with feed pressure at 1.0 bar and draw pressure at 0.2 bar. The membrane was replaced when changing draw solution type . Measurements with pure water feed were carried out for each draw solution type prior to simulate POME digestate feed water. Between each run with pure water feed, the membrane was flushed as described for fresh membranes. In between runs with simulated POME feed, membrane was cleaned by alternate runs of pure water, pH 10 NaOH solution and finally pure water, with each run lasting until after flushed water ran clear and for at least 15 minutes in each case.

Lignosulfonate concentrations were made up at 50, 100 and 150 g l^{-1}. The lower value was determined as concentrations below this value were not expected to give very high fluxes, particularly when using HA feed water. The high concentration value was selected, as dissolving greater quantities than this proved difficult in practise. NaCl draw solutions were used to allow comparisons with other FO studies, where NaCl is used as a standard. Concentrations were limited to 1.0M (58.44 g l^{-1}) due to our prior experience of problems with salt precipitation on the surface of this particular membrane at higher concentrations [21].

3.0 Results and Discussion

3.1 Freezing point osmometry measurement of solutions.

Freezing point osmometry was used to characterise osmotic concentration of relevant solutions in this study. POME digestate was found to have a value of 0.132 Osmol kg^{-1} (standard deviation ±0.00186). In addition, measurements were made of Na and Ca lignosulfonate solutions to allow calibration curves to allow determination of mass concentration and osmotic pressures of organic solutions from osmolality measurements (figure 2). In all cases the relationship between mass concentration and osmolality was highly linear with *y*-axis intercepts of approximately zero. From linear regression to the

HA curve, it can be determined that a concentration of HA of 66.2 g l^{-1} would have an osmolality equal to the POME digestate.

3.2 Determination of osmotic pressures from dead-end filtration

To verify the efficacy of determining osmotic pressure from dead end filtration flux rates, initial dead end filtration tests were carried out for pure water and 0.11 M sucrose and 0.05M raffinose at a range of applied pressures (figure 3). Values of J_w = 0 obtained from linear regression were 0.11, 2.64 and 1.23 bar for the water, sucrose and raffinose solutions respectively. For the sucrose and raffinose solutions this generated error values compared to values calculated from the van't Hoff equation of 1.51 % and 0.91 % respectively, suggesting this is a valid approach to osmotic pressure determination.

HA, Na Lig and Ca Lig solutions of various concentrations, as well as POME digestate were filtered at various pressures using a dead end filtration set-up. For the POME digestate (figure 4), extrapolation to the x-axis (i.e. J_w =0) gave an osmotic pressure value of 1.58 bar.

Osmotic pressure versus applied hydraulic pressure is plotted for Na and Ca lignosulfonates, as well as HA, in figure 5. As can be seen for the concentrations examined, there is a linear relationship between osmotic pressure and mass concentration, although the slopes for each lignosulfonate differ. The linear plots suggest that under these conditions the solutions behave as ideal solutions and the van't Hoff equation is in this case valid. For HA solutions, measurements at higher pressure for the 50 and 100 g l^{-1} concentrations deviated from this linear relationship, with flux becoming independent of applied hydraulic pressure, indicating concentration polarization was occurring [39], despite the relatively high stirrer speed (100 rpm). As a result, data taken at higher pressures was not used for these concentrations of HA. This behaviour was not observed for other solutions or lower concentrations of HA.

Osmotic pressure values for tested solutions plotted against mass concentration are shown in figure 6. As can be seen for the lignosulfonate and HA solutions linear fits, which approximately find the intercept at $y, x = 0$ were obtained. Construction of calibration curves of osmotic pressure versus measured osmolality (figure 7) allowed estimation of solution osmotic pressure from freezing point depression measurements directly without the need for knowledge of unknown sample parameters, such as the number averaged molecular weight.

It can be calculated that at a 2% by weight lignosulfonate solution suitable for spraying onto soils, osmotic pressures of 1.89 and 1.46 bar for Na Lig and Ca Lig respectively. The higher value for Na Lig is above that of the POME digestate suggesting that it is at least theoretically possible to achieve a 2% final lignosulfonate concentration from FO alone. However, to achieve high flux rates the draw solution concentration should be significantly higher than the feed osmotic pressure, so for practical purposes much stronger draw solutions would be used, needing further dilution before applying to plantation soils.

For Na Lig and Ca Lig solutions, the plots of osmotic pressure versus osmolality showed very similar linear fits with almost identical slopes and intercepts (figure 7). As accurate conversion of molal concentrations to molar concentration require solute molecular weight and solution density [40], the coincidence of these two curves suggest these values are very similar for Na and Ca lignosulfonate, as would be expected. For the humic acid solutions a linear fit provides a close approximation, but has a much steeper slope than observed for the lignosulfonate solutions. Interestingly, the steepness of the HA curve suggests that the osmotic pressure of the simulated POME digestate feed water is likely to have a higher osmotic pressure (4.67 bar instead of 1.67 bar) than the actual POME digestate, despite having an identical osmolality. This also demonstrates that accurate osmotic pressure values cannot be derived from measured osmolality values using an arbitrary conversion factor [27, 41], when the solution to be tested is not a simple solution.

3.3 FO flux measurements using pure water feed with various draw solutions.

Figure 8 shows measured water flux for pure water feed measured with different concentrations of NaCl, Na Lig and Ca Lig as draw solutions. It is apparent that much higher fluxes are observed when using NaCl as a draw agent than for the lignosulfonates, with Na Lig performing better than Ca Lig by approximately 2 LMH for each concentration examined. However, the shape of the flux versus concentration curves are very different for NaCl and the lignosulfonate solutions. For NaCl, the pure water flux increased rapidly with increasing concentration at lower concentrations. However, no further increase in flux was observed with increasing draw solution concentration above 50 g l^{-1}, with a maximum flux of 17.4 LMH. This is likely due to a combination of scaling and concentration polarization effects combined with increase in bulk feedwater concentration due to reverse diffusion of dissolved species. Scaling was not visible to the eye, although we have observed scaling previously with NaCl at these concentrations for a similar set-up [21]. Concentration polarization is another likely contributor to the flux reduction for NaCl. From the measured change in feed concentration, the greatest change in feed water osmotic pressure (after 30 min of operation with 1 mol l^{-1} NaCl draw solution) was calculated to be less than 0.01 bar. This change in osmotic pressure difference is insubstantial and would not have been enough to significantly reduce flux, leaving concentration polarization due to dilution of draw solution in the support layer and salt ions accumulating close to the feed side of the active layer as the most likely explanation. Flux rates and behaviour was slightly greater than our previously reported values for a similar set-up using NaCl draw with pure water feed [21], but the difference is likely to be due to some changes in the configuration, most notably the use of different membrane support materials compared with the previous work. In contrast to the observations for NaCl, for both lignosulfonate solutions, change in membrane water flux with concentration could be approximated by a linear fit, although it is unknown if a linear trend would be maintained at higher concentrations. Higher concentrations were not investigated due to the difficulty of dissolving lignosulfonates at higher concentrations. From linear regression of the lignosulfonate fluxes versus draw concentration it can be calculated that the maximum observed flux of 17.4 LMH

for NaCl draw solute would be achieved at concentrations of 347.7 and 474.6 gl^{-1} for the Na and Ca lignosulfonates respectively. This is more than double the concentrations examined here, and it cannot be guaranteed that these concentrations could be dissolved easily. In addition, it is quite possible that at those high concentrations of draw solute the viscosity of solutions is likely to increase to the point at which water permeability would be affected.

A major contributor to concentration polarization in FO applications is reverse solute flux, due to transport of salts across the membranes from the draw to the feed side. This leads to a build-up of dissolved species on the feed side close to the membrane active surface. This in turn can dramatically reduce the osmotic pressure difference across the active layer to a much lower value than the osmotic pressure difference between the bulk phases [42].

In addition to its effect on concentration polarization and water flux, for the dewatering of POME digestate, transport of salts across the membrane to the feed side are of a major concern. Contamination of concentrated organic solids remaining in the feed with inorganic salts is likely to preclude their potential re-use as organic fertilisers, particularly for Na$^+$ salts. As a result, for POME digestate dewatering, reverse solute flux needs to be minimised where the draw solution contains inorganic salts. Solute fluxes for all draw solutions with pure water feeds were calculated from equation 4 and are plotted in figure 9a. As can be seen, as well as having the highest water flux, the NaCl draw solutions exhibit the highest values for J_s, which increase with draw concentration. Values for Na and Ca Lig are much less, with Na Lig being lowest, and are relatively unchanged with concentration. It should be noted that for the lignosulfonate solutions, the relatively high molecular weight of lignosulfonate suggests that reverse solute flux in their cases is due to transport of the associated counter ions.

The specific flux ($J_{Specific} = J_s/J_w$) was also calculated (figure 9b) for each solution. This ratio is an indication of the efficiency of the FO process, inversely related to the selectivity of the membrane under the operating conditions considered [43]. $J_{Specific}$ was lowest for Na Lig draw solution, with the

optimum value being for this draw solute with a concentration of 150 g l^{-1}. This indicates that the highest concentration of Na Lig gives the best combination of low reverse solute flux with highest water flux. This again indicates that Na Lig as a draw solution is superior to either NaCl or Ca Lig for dewatering of POME digestate, due to low contamination of feed waters with salts and reasonable forward water flux values.

Change in flux rates over time were examined to look for possible fouling effects on the membrane (figure 10). In most cases, the flux was relatively steady, with some small fluctuations over time. This may represent errors due to shaking of the analytical balance caused by water flow in the tanks, or the occasional need to adjust the pressure to maintain the required value. However, for the NaCl feed at the 0.75 and 1.00 M solution some decrease was seen in the first 10 min before stabilising, although the magnitude of this decrease was not very large.

3.4 FO flux measurements using simulated POME digestate feed with various draw solutions.

FO flux measurements were repeated using NaCl, Na Lig and Ca Lig with feed solution consisting of aqueous HA to simulate POME digestate solution. Values of flux versus draw concentration are shown in figure 11. The behaviour of the various draw solutions was similar to that seen for pure water feed, but with a significantly lowered flux in all cases. This is to be expected due to the significantly decreased osmotic pressure difference across the membrane due to the higher chemical potential of the simulated POME digestate feed, compared with the pure water feed. Again, NaCl shows the highest flux, but it appears to plateau at draw concentrations above 50 g l^{-1}, with a maximum value observed at 7.1 LMH. For the lowest concentration of Ca Lig (50 g l^{-1}) negative flux values were observed, with the direction of flow from the draw to the feed side, with positive flux rates only observed at 100 g l^{-1} and above. The negative flux for the lowest concentration of CA Lig is unsurprising as the measured osmotic pressure of this solution was 3.20 bar, compared with the 4.67 bar osmotic

pressure of the HA feed solution, as calculated from the osmolality calibration curve. The 100 gl-1 Ca Lig solution had a measured osmotic pressure of 5.10 bar, which resulted in a small (0.7 LMH) forward water flux. Similarly, for the 50 gl^{-1} Na Lig solution an osmotic pressure of 5.10 bar was measured, with a forward flux of 0.1 LMH.

A calculation can be made using equation 2 to predict what the expected water flux would be in the case of a concentrated feed solution of known osmotic pressure if ideal behaviour is observed, compared with flux measurements made with pure water feed, assuming a reflection coefficient of 1:

$$J_{w2} = \frac{J_{w1}(\pi_{DS} - \pi_{FS})}{\pi_{DS}}$$

where J_{w1} and J_{w2} are flux values with pure water and concentrated feed solutions, π_{DS} and π_{FS} are osmotic pressures of draw and feed solutions respectively. Assuming a feed osmotic pressure of 4.67 bar, predicted and actual flux values as well as absolute deviation, are presented in table 2. As can be seen, not only are flux values much lower than predicted in the naïve ideal case, but deviations increase with draw concentration. This indicates significantly increased resistance to trans-membrane flow through mechanisms which may involve increased membrane resistance due to fouling, or concentration polarization effects.

Change in flux over time was observed for tests using simulated POME digestate feed water (figure 12). As can be seen, at the highest draw concentration for NaCl (1.0 M), flux rates declined over the first 20 minutes of operation, at which point the flux values were similar to that for the 0.75M NaCl draw solution. Flux rates were relatively stable for other draw concentrations. For Na Lig solutions flux was relatively stable over time, with small variations likely due to experimental error. For Ca Lig however, much greater variation in fluxes were observed over time.

Conclusions

We have investigated the feasibility of the use of lignosulfonate solution for the dewatering of POME digestate for resource recovery. Flux rates for Na Lig and Ca Lig were below that for NaCl feeds of similar mass concentrations, but reverse solute flux was also much lower. Na Lig showed better water flux and lower reverse solute flux than Ca Lig. For the situation here, reverse solute flux is doubly important through the need to avoid contaminating the concentrated feed with dissolved salts.

Direct measurement of osmotic pressure of organic solutions were made using a dead-end filtration method and compared with osmolality results from freezing point depression osmometry. It was found that the correlation between osmolality and osmotic pressure differed for different solutions. As such the simulated POME digestate had a higher pressure of 5.35 bar, compare with the 1.52 bar measured for POME, despite the solutions both having the same osmolality. As such the simulated POME feed was more comparable with an already somewhat concentrated POME digestate. FO experiments using HA made up to the same osmolality as the tested POME digestate showed the same pattern of behaviour for each draw solution as for pure water feed, but with lowered flux rates. Flux rates were lower for all draw solutions, compared with that calculated for ideal behaviour from solutions osmotic pressures and pure water flux values. This suggested that further factors came in to play restricting water flux, such as increased membrane resistance due to membrane fouling and decreased osmotic pressure across the membrane active layer due to concentration polarization effects. The better performance of the Na Lig draw solutions compared with Ca Lig and the much lower reverse solute flux compared with both NaCl and Ca Lig solutions, combined with the potential for no need for a second stage draw concentration step, which is usually the most energy costly part of the overall FO process, suggest that Na Lig has much potential to be developed as a draw agent for FO dewatering of POME digestate waste streams.

Acknowledgements

References

[1] P. Pacheco, S. Gnych, A. Dermawan, H. Komarudin, B. Okarda, The palm oil global value chain: Implications for economic growth and socialand environmental sustainability, CIFOR, 2017.

[2] O. Imoisi, G. Ilori, I. Agho, J. Ekhator, Palm oil, its nutritional and health implications, Journal of Applied Sciences and Environmental Management, 19 (2015) 127-133.

[3] A.Z. Abdullah, B. Salamatinia, H. Mootabadi, S. Bhatia, Current status and policies on biodiesel industry in Malaysia as the world's leading producer of palm oil, Energy Policy, 37 (2009) 5440-5448.

[4] A.B. Moreira, V.H. Perez, G.M. Zanin, H.F. de Castro, Biodiesel synthesis by enzymatic transesterification of palm oil with ethanol using lipases from several sources immobilized on silica–PVA composite, Energy & Fuels, 21 (2007) 3689-3694.

[5] Y. Basiron, Palm oil production through sustainable plantations, European Journal of Lipid Science and Technology, 109 (2007) 289-295.

[6] N.A. Bukhari, S.K. Loh, A.B. Nasrin, J.M. Jahim, Enzymatic Hydrolysate of Palm Oil Mill Effluent as Potential Substrate for Bioflocculant BM-8 Production, Waste and Biomass Valorization, (2018) 1-13.

[7] M.J. Chin, P.E. Poh, B.T. Tey, E.S. Chan, K.L. Chin, Biogas from palm oil mill effluent (POME): Opportunities and challenges from Malaysia's perspective, Renewable and Sustainable Energy Reviews, 26 (2013) 717-726.

[8] Y. Zhang, Y. Li, Q. Xiangli, C. Lina, N. Xiangjun, M. Zhijian, Z. Zhang, Integration of biological method and membrane technology in treating palm oil mill effluent, Journal of Environmental Sciences, 20 (2008) 558-564.

[9] A. Ahmad, S. Sumathi, B. Hameed, Coagulation of residue oil and suspended solid in palm oil mill effluent by chitosan, alum and PAC, Chemical Engineering Journal, 118 (2006) 99-105.

[10] W.L. Liew, M.A. Kassim, K. Muda, S.K. Loh, A.C. Affam, Conventional methods and emerging wastewater polishing technologies for palm oil mill effluent treatment: a review, Journal of Environmental Management, 149 (2015) 222-235.

[11] N.S. Zafisah, W.L. Ang, D.J. Johnson, A.W. Mohammad, N. Hilal, Effect of different filter aids used in cake filtration process on the removal of suspended solids in anaerobically digested palm oil mill effluent (POME), Desalination and water treatment, 110 (2018) 362-370.

[12] N. Akther, A. Sodiq, A. Giwa, S. Daer, H.A. Arafat, S.W. Hasan, Recent advancements in forward osmosis desalination: A review, Chemical Engineering Journal, 281 (2015) 502-522.

[13] D.L. Shaffer, J.R. Werber, H. Jaramillo, S. Lin, M. Elimelech, Forward osmosis: Where are we now?, Desalination, 356 (2015) 271-284.

[14] A. Achilli, T.Y. Cath, E.A. Marchand, A.E. Childress, The forward osmosis membrane bioreactor: A low fouling alternative to MBR processes, Desalination, 239 (2009) 10-21.

[15] T.Y. Cath, A.E. Childress, M. Elimelech, Forward osmosis: principles, applications, and recent developments, Journal of Membrane Science, 281 (2006) 70-87.

[16] A.J. Ansari, F.I. Hai, W.E. Price, J.E. Drewes, L.D. Nghiem, Forward osmosis as a platform for resource recovery from municipal wastewater - A critical assessment of the literature, Journal of Membrane Science, 529 (2017) 195-206.

[17] M. Elimelech, W.A. Phillip, The future of seawater desalination: energy, technology, and the environment, science, 333 (2011) 712-717.

[18] R.W. Field, J.J. Wu, Mass transfer limitations in forward osmosis: Are some potential applications overhyped?, Desalination, 318 (2013) 118-124.

[19] D.J. Johnson, W.A. Suwaileh, A.W. Mohammed, N. Hilal, Osmotic's potential: An overview of draw solutes for forward osmosis, Desalination, 434 (2018) 100-120.

[20] T. Alejo, M. Arruebo, V. Carcelen, V.M. Monsalvo, V. Sebastian, Advances in draw solutes for forward osmosis: Hybrid organic-inorganic nanoparticles and conventional solutes, Chemical Engineering Journal, 309 (2017) 738-752.

[21] W. Suwaileh, D. Johnson, N. Hilal, Brackish water desalination for agriculture: Assessing the performance of inorganic fertilizer draw solutions, Desalination, 456 (2019) 53-63.

[22] S. Zou, Z. He, Enhancing wastewater reuse by forward osmosis with self-diluted commercial fertilizers as draw solutes, Water research, 99 (2016) 235-243.

[23] P. Nasr, H. Sewilam, Investigating the performance of ammonium sulphate draw solution in fertilizer drawn forward osmosis process, Clean Technologies and Environmental Policy, 18 (2016) 717.

[24] S. Phuntsho, H.K. Shon, S. Hong, S. Lee, S. Vigneswaran, A novel low energy fertilizer driven forward osmosis desalination for direct fertigation: evaluating the performance of fertilizer draw solutions, Journal of Membrane Science, 375 (2011) 172-181.

[25] S. Phuntsho, H.K. Shon, T. Majeed, I. El Saliby, S. Vigneswaran, J. Kandasamy, S. Hong, S. Lee, Blended fertilizers as draw solutions for fertilizer-drawn forward osmosis desalination, Environmental science & technology, 46 (2012) 4567-4575.

[26] L. Chekli, Y. Kim, S. Phuntsho, S. Li, N. Ghaffour, T. Leiknes, H.K. Shon, Evaluation of fertilizer-drawn forward osmosis for sustainable agriculture and water reuse in arid regions, Journal of Environmental Management, 187 (2017) 137-145.

[27] J. Duan, E. Litwiller, S.-H. Choi, I. Pinnau, Evaluation of sodium lignin sulfonate as draw solute in forward osmosis for desert restoration, Journal of Membrane Science, 453 (2014) 463-470.

[28] J.S. Vinod, B. Indraratna, M.A. Al Mahamud, Stabilisation of an erodible soil using a chemical admixture, (2010).

[29] D.P. Alazigha, J.S. Vinod, B. Indraratna, A. Heitor, Potential use of lignosulfonate for expansive soil stabilisation, Environmental Geotechnics, (2018) 1-9.

[30] A.H. Vakili, M. Kaedi, M. Mokhberi, M.R. bin Selamat, M. Salimi, Treatment of highly dispersive clay by lignosulfonate addition and electroosmosis application, Applied Clay Science, 152 (2018) 1-8.

[31] A.E. Hartemink, Soil erosion: perennial crop plantations, Encyclopedia of soil science, (2006) 1613-1617.

[32] S. Sahat, Z. Yusop, M. Askari, A. Ziegler, Estimation of Soil Erosion Rates in Oil Palm Plantation with Different Land Cover, in: IOP Conference Series: Materials Science and Engineering, IOP Publishing, 2016, pp. 012086.

[33] W. Hanjie, P. de Vries FRITS, J. Yongcan, A win-win technique of stabilizing sand dune and purifying paper mill black-liquor, Journal of Environmental Sciences, 21 (2009) 488-493.

[34] J. LI, A field experimental study of lignin sand stabilizing material (LSSM) extracted from spent-liquor of straw pulping paper mills, Journal of Environmental Sciences, 17 (2005) 650-654.

[35] L.X.J.Y.Y. Yiqin, C.Y.L. Zhongzheng, Application of Lignin Sand-Fixer to Vegetation Restoration in Desertificated Areas [J], Scientia Silvae Sinicae, 4 (2005).

[36] T.E. Sweeney, C.A. Beuchat, Limitations of methods of osmometry: measuring the osmolality of biological fluids, American Journal of Physiology-Regulatory, Integrative and Comparative Physiology, 264 (1993) R469-R480.

[37] H. Nabetani, M. Nakajima, A. Watanabe, S.-i. Ikeda, S.-i. Nakao, S. Kimura, Development of a new type of membrane osmometer, Journal of chemical engineering of Japan, 25 (1992) 269-274.

[38] N.C. Nguyen, H.T. Nguyen, S.-T. Ho, S.-S. Chen, H.H. Ngo, W. Guo, S.S. Ray, H.-T. Hsu, Exploring high charge of phosphate as new draw solute in a forward osmosis–membrane distillation hybrid system for concentrating high-nutrient sludge, Science of The Total Environment, 557 (2016) 44-50.

[39] R. Ghosh, Principles of bioseparations engineering, World Scientific Publishing company, 2006.

[40] H.-J. Bart, Reactive Extraction, Springer, 2001.

[41] Q. Ge, J. Su, G.L. Amy, T.-S. Chung, Exploration of polyelectrolytes as draw solutes in forward osmosis processes, Water research, 46 (2012) 1318-1326.

[42] J.R. McCutcheon, M. Elimelech, Influence of concentrative and dilutive internal concentration polarization on flux behavior in forward osmosis, Journal of Membrane Science, 284 (2006) 237-247.
[43] N.T. Hancock, T.Y. Cath, Solute coupled diffusion in osmotically driven membrane processes, Environmental science & technology, 43 (2009) 6769-6775.

Figure Captions

Figure 1: Diagram showing FO system configuration. Draw side is shown in blue, feed side in red.

Figure 2: Change in solution osmolality with mass concentration.

Figure 3: Change in flux versus applied hydraulic pressure for pure water and solutions of the sugars sucrose and raffinose.

Figure 4: Change in flux for dead end filtration of POME digestate. Zero net flux relates to sample osmotic pressure of 1.58 bar.

Figure 5: Flux rates versus pressure for dead end filtration of a) Na Lignosulfonate; b) Ca Lignosulfonate; c) Humic Acid

Figure 6: Measured osmotic pressure versus mass concentration for lignosulfonate solutions and humic acid.

Figure 7: Plot of measured osmotic pressure versus osmolality values obtained from freezing point depression measurements.

Figure 8: Measured water flux values obtained using NaCl, Ca lignosulfonate, Na lignosulfonate for pure water feed.

Figure 9: a) Reverse solute flux and b) specific flux for each draw solution examined.

Figure 10: Change in membrane water flux over time for pure water feed solution with: a) NaCl draw solution; b) Na lignosulfonate draw solution; c) Ca Lignosulfonate draw solution.

Figure 11: Measured water flux values obtained using NaCl, Ca lignosulfonate, Na lignosulfonate for simulated POME digestate feed.

Figure 12: Change in membrane water flux over time for simulated POME digestate feed solution with: a) NaCl draw solution; b) Na lignosulfonate draw solution; Ca Lignosulfonate draw solution.

**Figures**
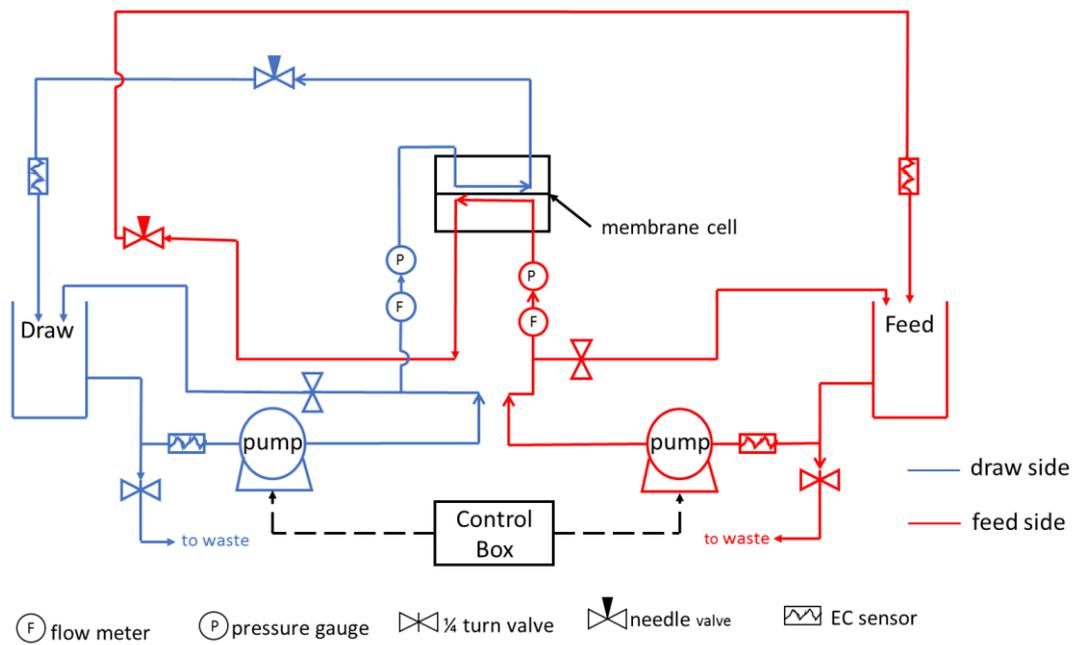

Figure 1
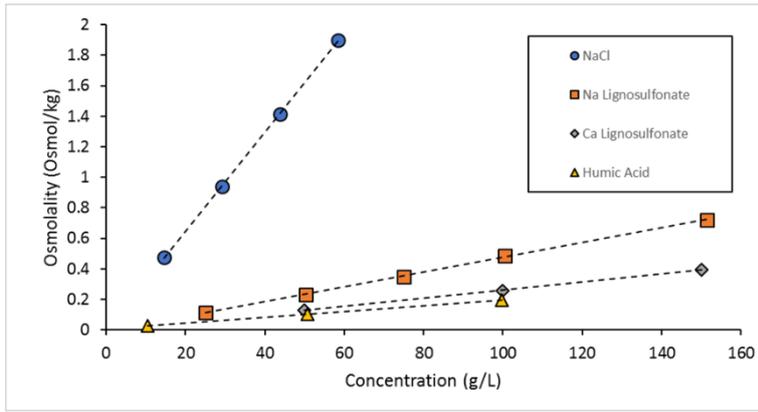
Figure 2
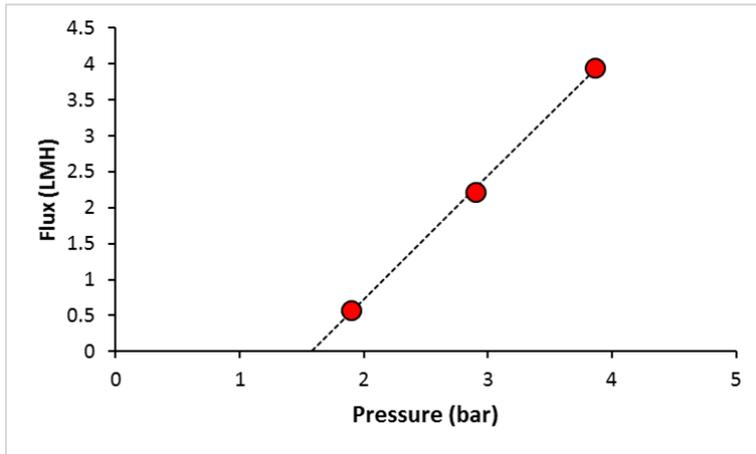
Figure 3
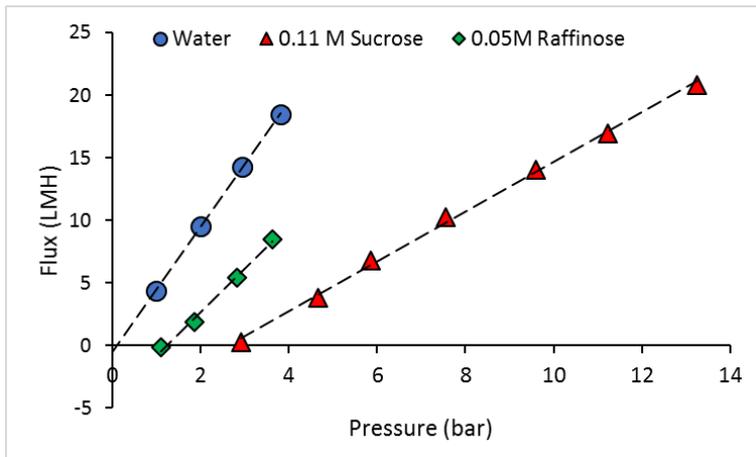
Figure 4
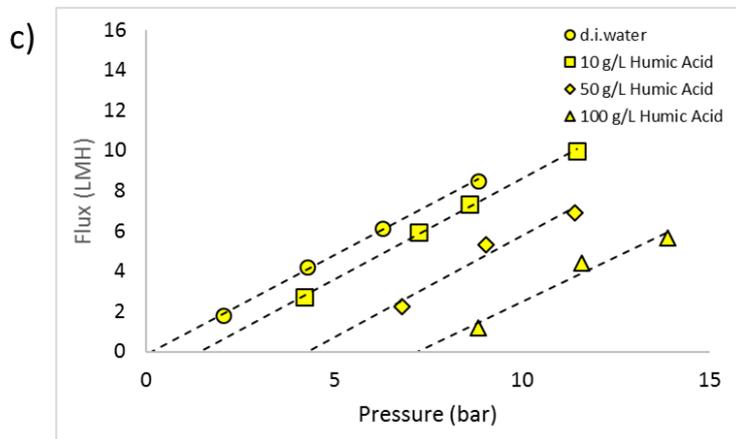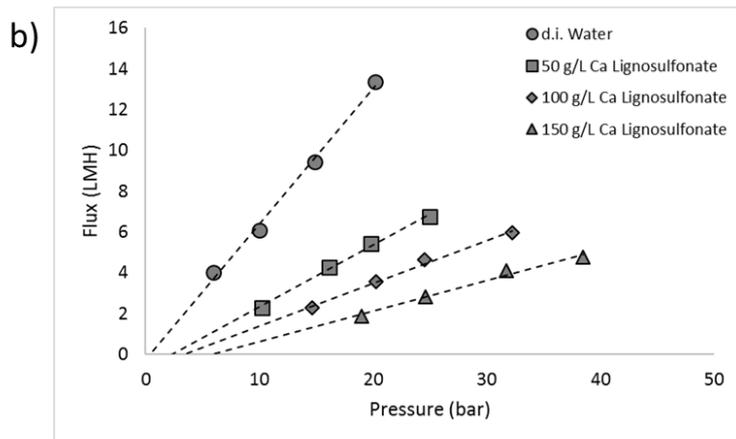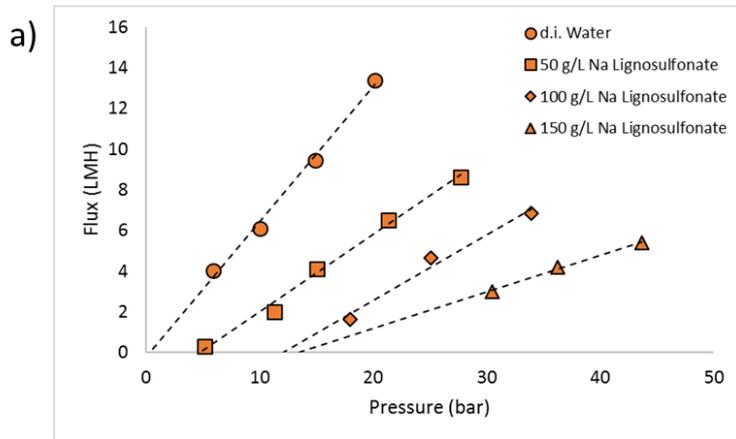
Figure 5
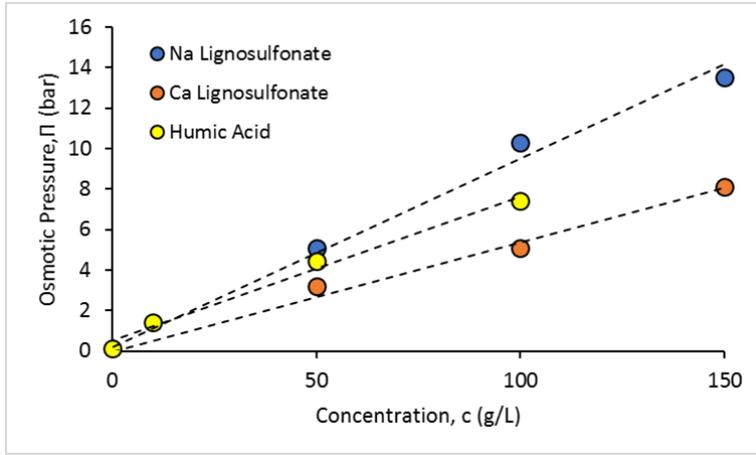
Figure 6
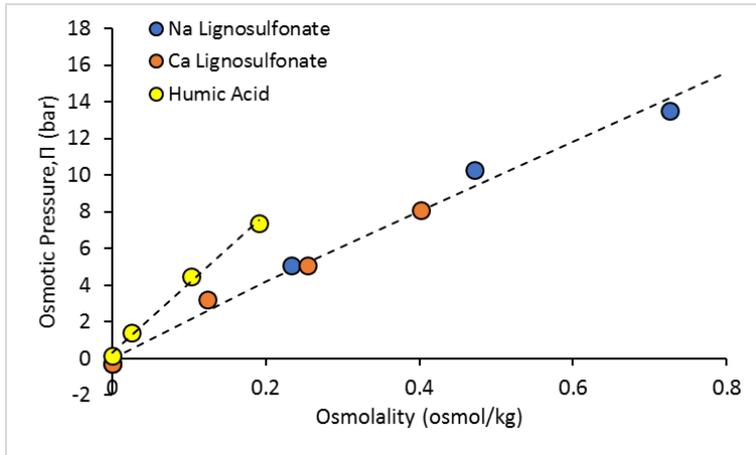
Figure 7
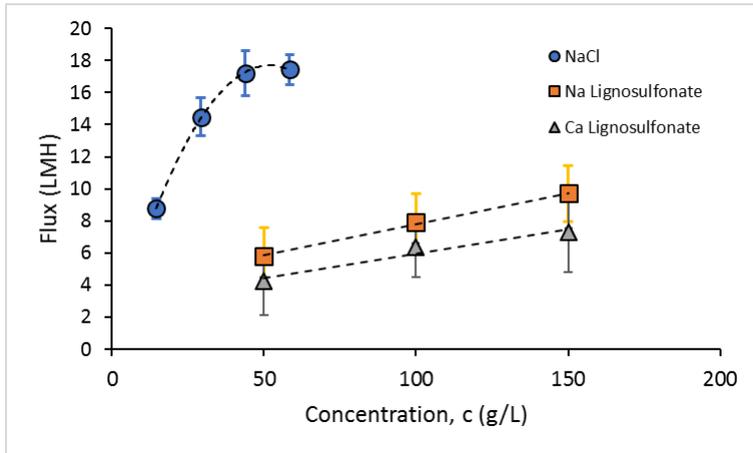
Figure 8
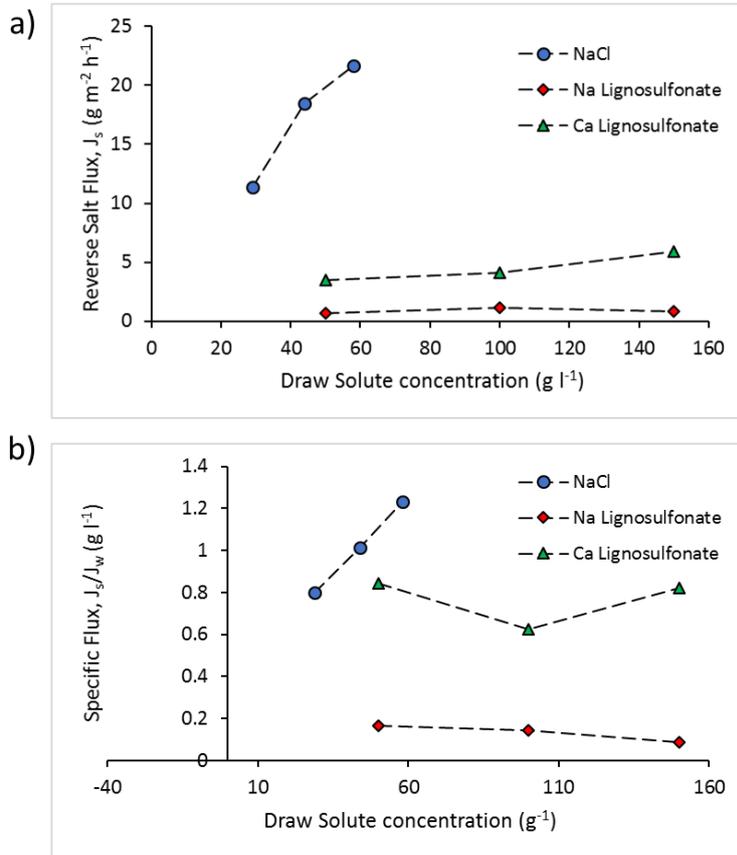
Figure 9
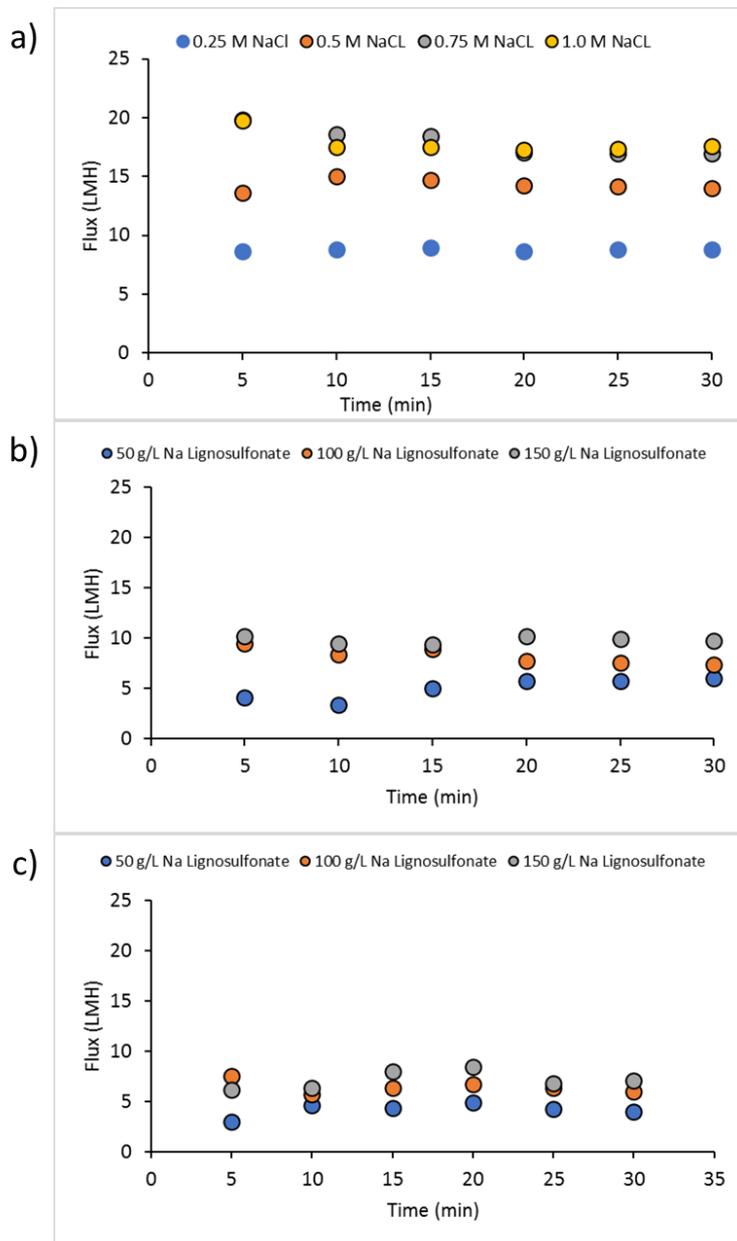
Figure 10
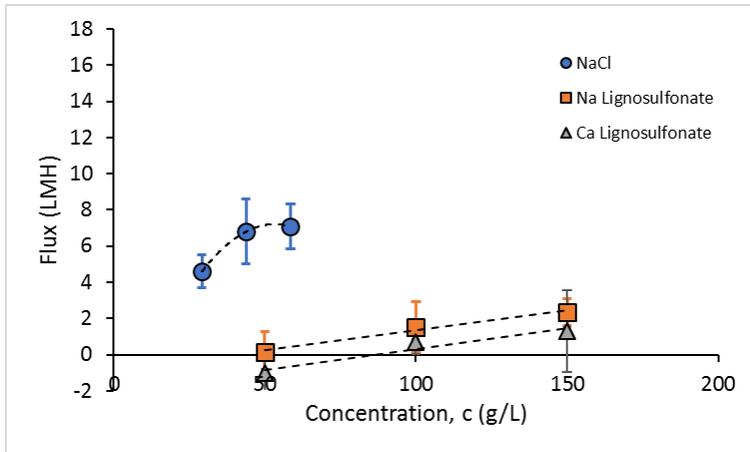
Figure 11
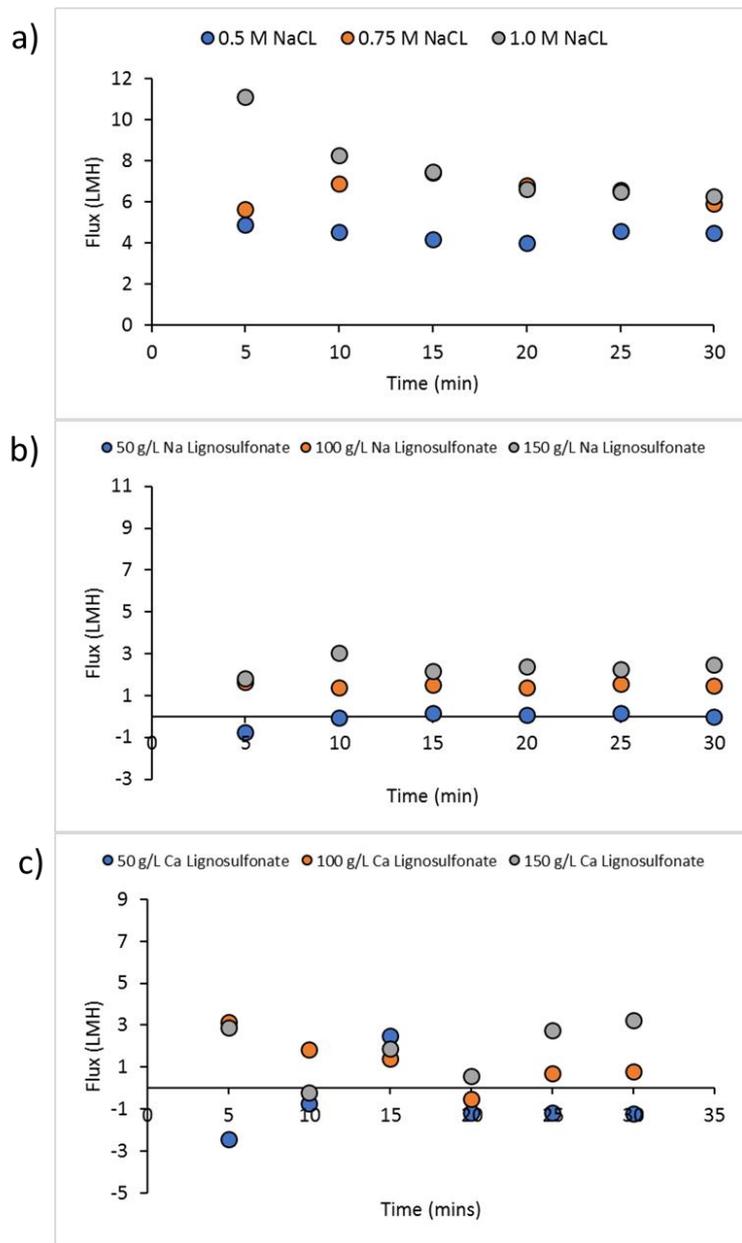
Figure 12

Tables

Table 1: Parameters for anaerobically digested POME. Parameters marked * obtained from UV/Vis spectroscopy using calibration curves of known concentrations. All other values previously reported in [11].

Table 2: Predicted and actual fluxes from simulated POME digestate feed for various draw solutions feed (DS).

Parameters	Digestate POME
pH	7.64
COD (mg/L)	6467
Total suspended solid (mg/L)	3457
Turbidity (NTU)	1303
Nitrogen Ammonia (mg/L)	342
Phosphorus (mg/L)	242
Humic acid (mg/L) *	702.3
Sodium (mg/L) *	82.9
Calcium (mg/L) *	193.1

Table 1

	Concentration	J_{w1}	J_{w2} (Actual)	J_{w2} (Predicted)	Difference
DS	(g/l)	(LMH)	(LMH)	(LMH)	
NaCl	29.22	14.5	4.6	11.7	-7.1
	43.83	17.2	6.8	15.0	-8.2
	58.44	17.4	7.1	15.8	-8.7
Na Lig	50	5.8	0.1	0.5	-0.4
	100	7.9	1.5	4.3	-2.8
	150	9.7	2.4	6.4	-4.0
Ca Lig	50	4.2	-1.0	-1.9	0.9
	100	6.4	0.7	0.5	0.1
	150	7.3	1.3	3.1	-1.8

Table 2